# Extensive fire-driven degradation in 2024 marks worst Amazon forest disturbance in over two decades

Clément Bourgoin[1], René Beuchle[1], Alfredo Branco[1], João Carreiras[2], Guido Ceccherini[3], Duarte Oom[1], Jesus San-Miguel-Ayanz[1], Fernando Sedano[1]

[1]European Commission, Joint Research Centre (JRC), Ispra, 21027, Italy
[2]VASS Italy, Torino, 10100, Italy
[3]Independent researcher providing service to the Joint Research Centre (JRC), European Commission, Ispra, 21027, Italy

*Correspondence to*: Clément Bourgoin (clement.bourgoin@ec.europa.eu)

**Abstract.** The Amazon rainforest, historically fire-resistant, is experiencing an alarming increase in wildfires due to climate extremes and human activity. The 2023/2024 drought, surpassing previous records, combined with forest fragmentation, has dramatically heightened fire vulnerability. Analysing the Tropical Moist Forest (TMF) and Global Wildfire Information System (GWIS) datasets, we found a 152% surge in forest disturbances from deforestation and degradation in 2024, reaching a two-decade peak of 6.64 million hectares. Forest degradation, particularly large-scale degradation linked to fires, increased by over 400%, largely exceeding deforestation. Brazil and Bolivia experienced the most severe impacts, with Bolivia seeing 9% of its intact forest burned in 2024. Fire-driven forest degradation in the Pan-Amazon released 791 ± 86 Mt $CO_2$ (million tons of carbon dioxide equivalent, ±1 standard deviation) in 2024—a seven-fold increase compared to the previous two years—surpassing emissions from deforestation. The escalating fire occurrence, driven by climate change and unsustainable land use, threatens to push the Amazon towards a catastrophic tipping point. Urgent, coordinated efforts are crucial to mitigate these drivers and prevent irreversible ecosystem damage.

## 1 Introduction

The Amazon's humid forests, once resistant to fire due to their high humidity and regular rainfalls, are undergoing an alarming and rapid transformation. The unprecedented 2023/2024 drought, which shattered the 2010 and 2015/2016 records with its dramatic precipitation deficit and prolonged, intense heat waves (Kornhuber et al., 2024, Marengo et al., 2024), has severely stressed the region's delicate ecological balance. This has resulted in diminished surface water resources, reduced soil moisture, and stressed vegetation, creating conditions that significantly elevate the likelihood and severity of forest fires (Barlow et al., 2020). This already precarious situation is further compounded by the forest's degraded state—a consequence of extensive deforestation and habitat fragmentation, selective logging, and past fire events—leaving it increasingly susceptible to future, potentially catastrophic wildfires (Bourgoin et al., 2024). This degraded state also sets in motion a series of detrimental feedback loops: the increased tree mortality due to edge effects acts as readily available fuel for fires, while fragmentation

facilitates greater access for hunting and resource extraction, both of which contribute directly to tree mortality and heightened fire incidence (Matricardi et al., 2012, Condé et al., 2019).

Natural fires, such as those caused by lightning, are extremely rare in the Amazon. Most fire ignitions in the Amazon result from human activity. Among them, "escape fires" are fires accidentally spreading into neighbouring forests from recently cleared deforested land or burned pastures and causing forest degradation (Cano-Crespo et al., 2015), or are deliberately set to pave the way for potential future illegal deforestation (Andela et al., 2022). The consequences of forest fires are multifaceted, directly harming plant and animal life, affecting the integrity of once-intact forests, and causing further damage to already degraded areas (Lapola et al., 2023). Recent degradation from fire shows a 60% decrease in aboveground biomass density compared to adjacent intact forests, releasing substantial greenhouse gases and accelerating global warming (Bourgoin et al., 2024). Forest fires also have severe implications for indigenous peoples, who face the threat of losing intact forest within their territories and experience severe respiratory health impacts from smoke exposure, often more so than other residents of the Amazon (Rorato et al., 2022).

As Amazon fire threats grow, rapid and accurate detection is paramount. Distinguishing forest degradation fires from agricultural fires is key to assessing impacts on people, ecosystems, and climate, and to developing effective mitigation measures. To address this need, we analysed the Tropical Moist Forest (TMF) dataset, updated through 2024 (Vancutsem et al. 2021). This dataset, leveraging the Landsat archive from 1990 onwards, identifies forest disturbances, classifying them as either deforestation or degradation (Vancutsem et al., 2021, see the Appendix for more details). It further classifies degradation into small-scale (a proxy for windthrow and selective logging) and large-scale events (a proxy for forest fire and drought). To enhance our understanding of fire-driven degradation, we integrated the Global Wildfire Information System (GWIS) burnt area data, which relies on Moderate-Resolution Imaging Spectroradiometer (MODIS) and Visible Infrared Imaging Radiometer Suite (VIIRS) thermal anomalies from 2012-2024 (San-Miguel et al., 2023). We estimated carbon dioxide ($CO_2$) emissions from fire-driven degradation and deforestation, along with their associated uncertainties, following the IPCC (2006) guidelines and incorporating the ESA CCI 2021 Above Ground Biomass dataset (Santoro et al., 2024).

## 2 Results

Our results show that the area of the Pan-Amazon region affected by forest disturbances dramatically increased by 152% from 2023 to 2024, reaching a two-decade peak of 6.64 million hectares (Mha) (Figure 1a). Despite a 20% decrease in deforestation in 2024 compared to the 2019-2023 average, forest degradation surged by over 400%, generally becoming increasingly prominent and surpassing deforestation by 1.3, 1.7, and 4.2 times in the 2010, 2016, and 2024 extreme climatic events. Large-scale degradation totaled 3.31 Mha in 2024, representing a 1077% increase compared to the annual average for the 2019–2023

period. This coincided with a 1461% increase in burned forest area, totaling 3.56 Mha, 80% of which overlaps with TMF-large scale degradation (more details on the integration of TMF-GWIS datasets in Section A3).

Brazil suffered the largest absolute large-scale degradation in 2024 (1.66 Mha, or 50% of Pan-Amazon large-scale degradation). Bolivia experienced the highest relative percentage with 9% of its remaining intact forest burned, compared to 0.6% in Brazil (Figure 1b, Figure A1). To a lesser extent, the 2024 increase in forest fires was also observed in countries historically less affected, such as the Guiana Shield countries and Venezuela, where large-scale degradation was 6 and 19 times higher than the previous 5-year average, respectively (see the Appendix for more details and Figure A2).

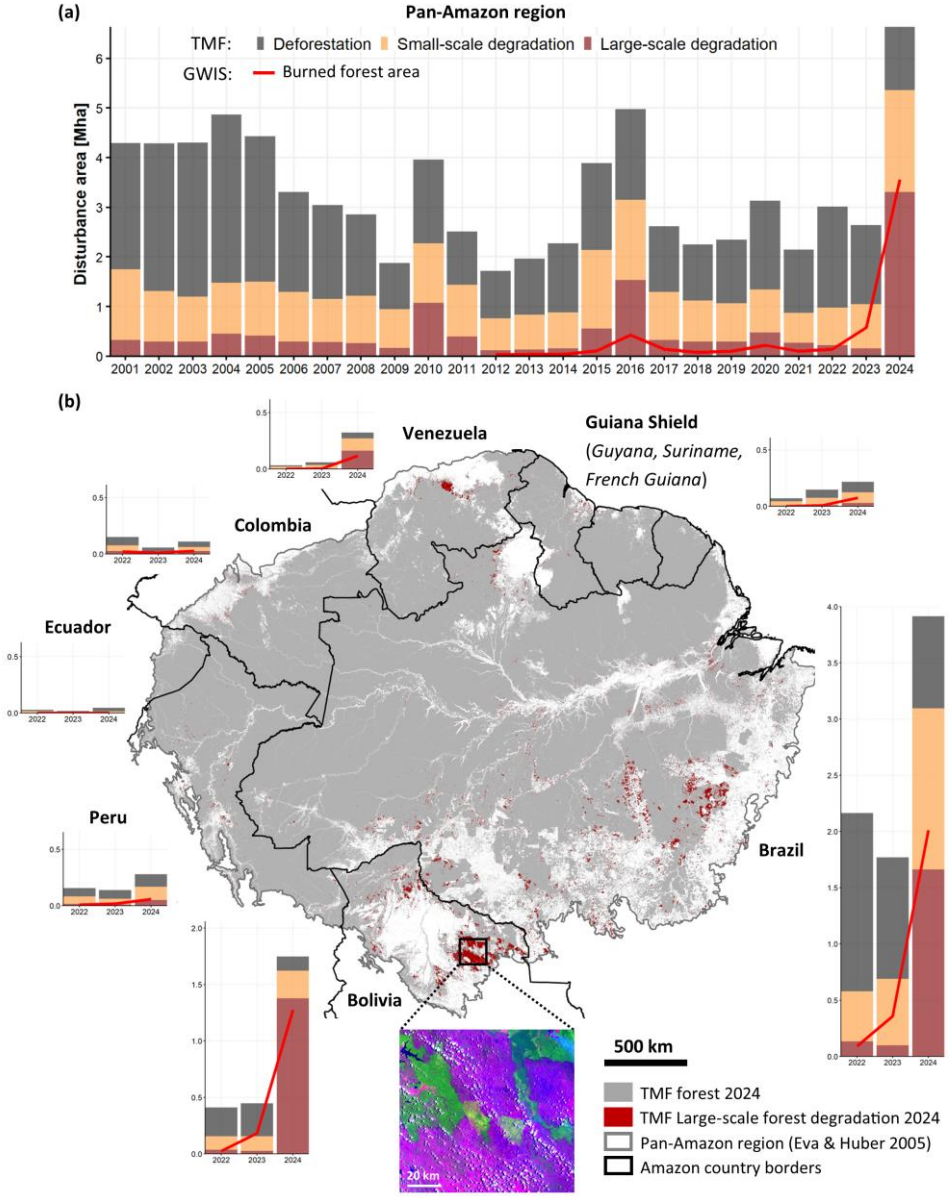


**Figure 1:** (a) Pan-Amazon Tropical Moist Forest (TMF) Disturbances (2001-2024), including deforestation (dark grey), small-scale degradation (orange), and large-scale degradation (dark red) from TMF. Burned forest area (red line) represents GWIS thermal anomalies overlapping with TMF historical degradation and 2023-2024 TMF disturbances, where GWIS detected the fire in the same or previous year. (b) Tropical Moist Forest Map: Large-scale TMF 2024 forest degradation and recent country forest disturbances (legend and units as panel a). The inset shows Landsat-8 imagery (courtesy of the U.S. Geological Survey USGS/NASA), with burn scars in purple and undisturbed forest in green (Oct. 21, 2024; RGB: bands 6, 5, 4). The Pan-Amazon region from Eva & Huber 2005 comprises the regions 'Amazonia stricto sensu' and 'Guiana'. Figures A1-A3 provide further details on TMF-GWIS data integration and on absolute/relative forest disturbances at the country-level.

Burned forests resulting from fire-driven degradation in the Pan-Amazon region released an estimated 791 ± 86 Mt $CO_2$ (million tons of carbon dioxide equivalent, ±1 standard deviation) in 2024—approximately seven times higher than the annual average of the previous two years (117 ± 13 Mt $CO_2$; see Figure 2). Brazil was the largest contributor, accounting for 61% of these emissions, followed by Bolivia with 32%. In contrast, emissions from deforestation declined from 1,044 ± 65 Mt $CO_2$ in 2022 to 625 ± 38 Mt $CO_2$ in 2024. Altogether, emissions from deforestation and fire-driven degradation totaled 1,416 ± 108 Mt $CO_2$ in 2024, with burned forest emerging as the dominant source. Comparatively, the latest publication of the Global Carbon Budget (Friedlingstein et al., 2025) also refers to a massive increase in emissions from deforestation and degradation fires in South America in 2024, from 445 Mt $CO_2$ in 2023 to 1,227 Mt $CO_2$ in 2024, mostly driven by the unusual dry conditions linked to El Niño.

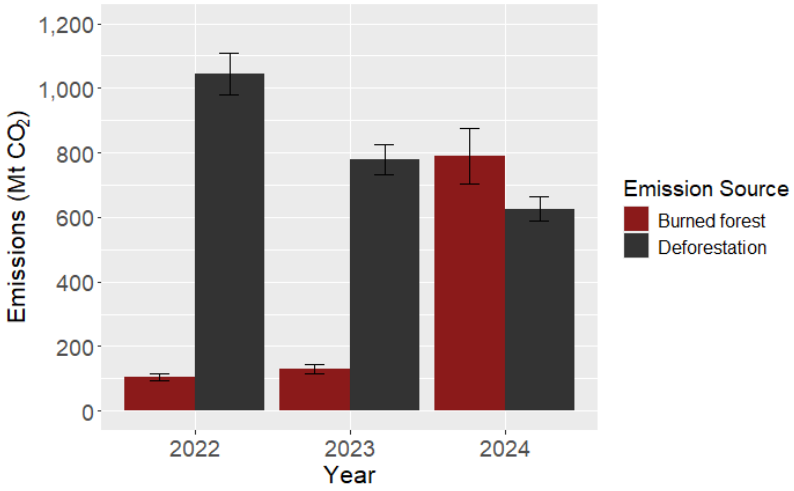


**Figure 2:** Pan-Amazon emissions from deforestation and fire-driven degradation in 2022-2024. Emissions from small-scale degradation processes (e.g., selective logging) or from disturbances in areas where GWIS thermal anomalies do not overlap with TMF forest degradation are not included in this analysis. Bars represent the mean values, and vertical error bars indicate the standard deviations, both derived from combining uncertainties using Monte Carlo simulation.

## 3 Discussion and conclusions

Our analysis presents findings with certain inherent limitations that should be considered during interpretation. The TMF dataset employed may have a tendency to underrepresent the extent of small-scale forest degradation (<0.09 ha), particularly that resulting from edge effects, selective logging and low-intensity fire events. These types of non-permanent disturbances can have considerable ecological consequences that may not be fully captured in the data (Bourgoin et al., 2024). Furthermore, differentiating between disturbances caused by degradation processes and those resulting from deforestation posed a challenge, specifically in the context of the 2024 data, as indicated by Vancutsem et al. (2021) due to lack of historical depth in detecting forest recovery following degradation. This overlap in observational characteristics could introduce some level of uncertainty in the precise categorization of forest change. While these limitations suggest a potential for underestimation of the overall impact, our estimates regarding the general scale of the area affected by fires are considered reasonably consistent and remain

conservative. The broad magnitude of the impacted area is unlikely to be drastically altered by these factors, suggesting that fire remains a significant driver of landscape change within the study area.

In 2024, forest fires became the leading cause of overall forest disturbance across the Pan-Amazon region. These fires not only triggered significant immediate carbon losses but also set in motion long-term ecological degradation. This degradation is marked by shifts in forest composition—driven by the limited evolutionary adaptations of Amazonian species to fire—along with persistently high rates of tree mortality. As a result, affected forests may act as a net source of carbon emissions for up to seven years or more after the fire (Lapola et al., 2023). Climate change, unsustainable land use, and increased forest vulnerability are fueling a self-reinforcing cycle of escalating fire occurrence and intensity in the Amazon region. This destructive synergy undermines regional forest conservation goals, driving significant forest degradation, particularly during extreme weather events, and potentially leading to permanent shifts in precipitation patterns, including intensified dry seasons along the Amazon's southern, eastern and northern borders (Hirota et al., 2021).

The 2024 data from Brazil, Bolivia and Venezuela highlights the Amazon's rapidly decreasing resilience. The uneven distribution of degradation, coupled with the rising frequency and intensity of forest fires, necessitates robust data-driven mapping approaches and standardized reporting systems to facilitate effective regional coordination and response (Melo et al., 2023). To address these challenges, it is crucial to prioritize areas of intervention and develop targeted strategies for reducing deforestation and forest degradation (Lapola et al., 2023). If left unchecked, current trends will push the Amazon forest towards a catastrophic tipping point, irreparably damaging the ecosystem and global climate stability (Flores et al., 2024). Therefore, immediate action is essential to mitigate the underlying drivers of forest fires and prevent the crossing of this critical threshold.

## 4 Appendix A

### A1 Tropical Moist Forest dataset

The Tropical Moist Forest (TMF) dataset provides a comprehensive, wall-to-wall mapping of global tropical humid forest cover dynamics from 1990 to 2024 at 30m spatial resolution, using the entire Landsat archive to detect both permanent and temporary forest disturbances. The performance of disturbance detection in Latin America results in 7.1% omissions, 12.8% commissions and 91% overall accuracy (see Table S3 from Vancutsem et al., 2021).

The TMF system enables analytical separation of forest degradation and deforestation on an annual basis by recording disturbance event timing with daily temporal resolution, using duration and recurrence as proxies to separate distinct impacts of land use change (i.e. deforestation) from structural/functional alterations (i.e. degradation) within forested land (Bourgoin et al., 2024, Beuchle et al., 2021).

Degraded forests are forests that experienced up to three short-duration disturbance events between 1990 and 2023. These short-term events are characterized by a maximum duration of 900 days during which tree foliage cover is absent within a Landsat pixel and followed by forest recovery signal (Vancutsem et al., 2021). To qualify as separate events, disturbances must be separated by at least two years without any detected disturbances. If more than three of such events occur, the pixel is classified as deforestation, with the year of deforestation assigned to the start of the first observed disturbance. For 2024, the classification between degradation and deforestation is based on the ratio of valid observations (i.e. pixels free of clouds, haze, and cloud shadows) to observed disturbance events given the insufficient historical depth to determine disturbance permanence. Key drivers of forest degradation include selective logging, wildfires, and natural disturbances such as windthrow and prolonged drought (Vancutsem et al., 2021).

An automated 3x3 pixel moving window filter was applied to each new forest degradation event, classifying small, isolated patches (~<0.8ha) associated with log landings, felling gaps, and logging roads (Lima et al., 2020) separately from larger, contiguous patches indicative of fire scars and drought (Morton et al., 2011).

Deforestation is defined as the conversion of an undisturbed or previously degraded forest into another land cover type, indicated by either a single disturbance event lasting more than 900 days or by more than three short-term disturbance events. In both cases, the year of deforestation is assigned to the first year of the relevant disturbance sequence and is mostly driven by agricultural, infrastructure and mining expansion.

**A2 Global Wildfire Information System dataset**

The Global Wildfire Information System (GWIS) is a joint initiative of the Group on Earth Observations (GEO) and the Copernicus Work Programs that integrates existing information sources at regional and national levels in order to provide a comprehensive view and evaluation of fire regimes and their impacts at global level.

The GWIS system is an ecosystem of Geographic Information System applications used to monitor wildfires globally in near real-time. The core of the system is the Burned Area Near Real Time dataset (GWIS BA NRT), which contains geolocated wildfire events along with associated metadata such as polygons, start and end dates and various ancillary attributes.

This dataset is derived from thermal anomalies detected by two satellite-based sensors: MODIS (Justice et al., 2002) (on board the TERRA and AQUA satellites) and VIIRS (Schroeder et al., 2014) (on board the SUOMI/NPP, NOAA20 and NOOA21 satellites).

The thermal anomalies covering the entire globe are obtained from the Fire Information for Resource Management System (FIRMS) near real-time dataset, and stored in a PostGIS database with their geolocation, acquisition date and other ancillary data unrelated to this topic.

The thermal anomalies are grouped based on their spatial and temporal proximity using the “Spatio-Temporal Density-Based Spatial Clustering of Applications with Noise” algorithm (ST-DBSCAN, Birant et al., 2007). The algorithm groups data points into clusters based on their spatio-temporal density, which is calculated using the following parameters: ε (i.e. the maximum

spatial distance), εt (i.e. the maximum temporal distance) and minPts (i.e. the minimum number of elements to start a cluster). Points that do not meet clustering criteria are labelled as noise. For each identified cluster, a circular buffer of 500m radius is created around each thermal anomaly. These buffers are then merged to create a polygon that approximates the area of the event. The earliest acquisition date among the anomalies defines the start of the fire event, while the latest defines the end.

The dataset used in this study includes detections from AQUA, TERRA, and SUOMI/NPP satellites, covering the period from 2012 onwards. Based on previous analyses, the clustering parameters applied were: ε=1.1km, εt=72h, minPts=4. This means each fire cluster included at least four thermal anomalies, and there were less than 1.1 km and 72 hours between neighboring anomalies. For this analysis, all the fire events falling in the Pan-Amazon region from Eva & Huber 2005 have been selected from the GWIS dataset for the years 2012 to 2024. This subset includes approximately 553 thousand clusters/burnt area events, with a cumulative burned area of around 250 million ha.

**A3 Integration of TMF-GWIS datasets**

To isolate burned forest area from GWIS thermal anomaly detections, we performed several spatial and temporal operations using the TMF dataset. A thermal anomaly detected by GWIS was considered burned forest only when the following conditions were met:

- Spatial overlap with TMF forest degradation (2012-2022). The anomaly had to intersect areas classified as forest degradation in the TMF dataset during the 2012–2022 period. This corresponds to short-duration disturbances, specifically 1 to 3 events, each lasting less than 900 days (see section A1 for details). GWIS detections within TMF-classified undisturbed forest were excluded from analysis. This step aims to address potential overestimations in GWIS fire detection due to its clustering and buffering approach (see section A2), as well as potential underdetections in TMF, particularly of small-scale events (<0.09ha) or those without significant canopy change (e.g., understory fires). Conclusive analysis of these cases requires independent validation, which is beyond this paper's scope, thus our results remain conservative. GWIS detections occurring on land classified by TMF as deforested or as other land cover (including areas deforested before 1990) were excluded. These areas are generally associated with deforestation-related fires (e.g., burning debris) or agricultural burning and fall outside the scope of our analysis focused on forest degradation.
- Temporal consistency with TMF degradation timing. The fire had to occur either in the same year as the TMF-recorded degradation or the preceding year. This temporal buffer accounts for potential delays in TMF detection due to Landsat's temporal resolution and important cloud cover in some parts of the Amazon region.
- Overlap with TMF forest disturbance (2023-2024). For the 2023–2024 period, anomalies were required to overlap with areas classified as forest disturbance in TMF. This adjustment acknowledges the current uncertainty in TMF's ability to distinguish between degradation and deforestation during this recent timeframe.

The application of these filters resulted in the exclusion of most GWIS thermal anomaly detections (Figure A3, panel a), with only 13.7% of the original dataset remaining. This remaining subset corresponds to approximately 14 million hectares of burned forest resulting from fire-driven degradation in Amazonian tropical moist forests. The trend of increasing burned forest area from 2012 to 2024 across different Pan-Amazonian land cover types is shown in Figure A3, panel b.

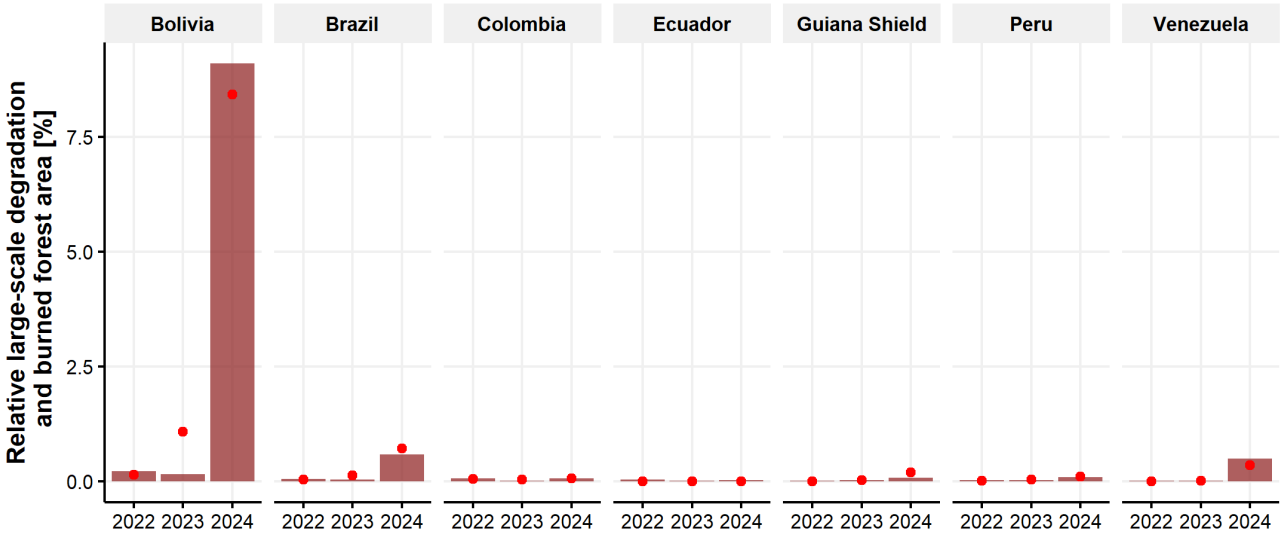


**Figure A1:** Large-scale degradation relative to intact forest area from TMF (bars) at the country-level within the Pan-Amazon region. Red dots indicate the burned area of tropical moist forest from TMF-GWIS integration related to the intact forest area from TMF.

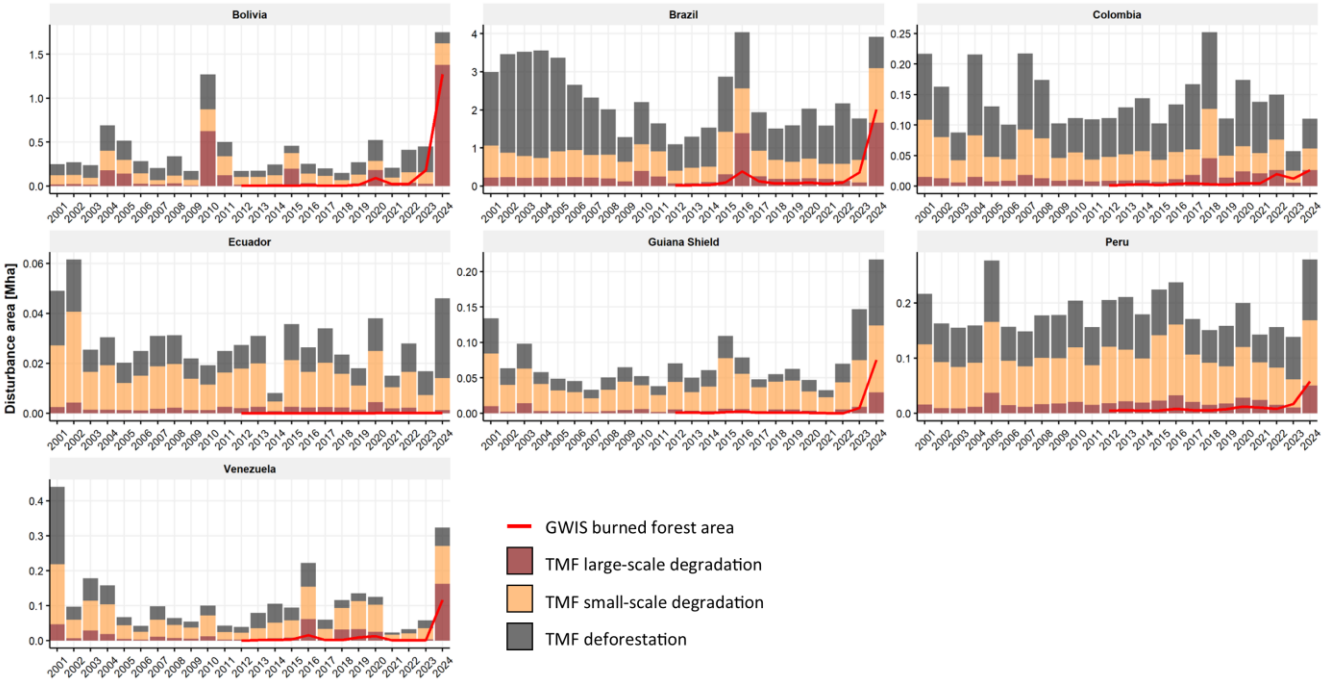


**Figure A2:** Amazonian forest disturbances from TMF (2001-2024) and burned forest area from TMF-GWIS integration (2012-2024) at country-level.

210

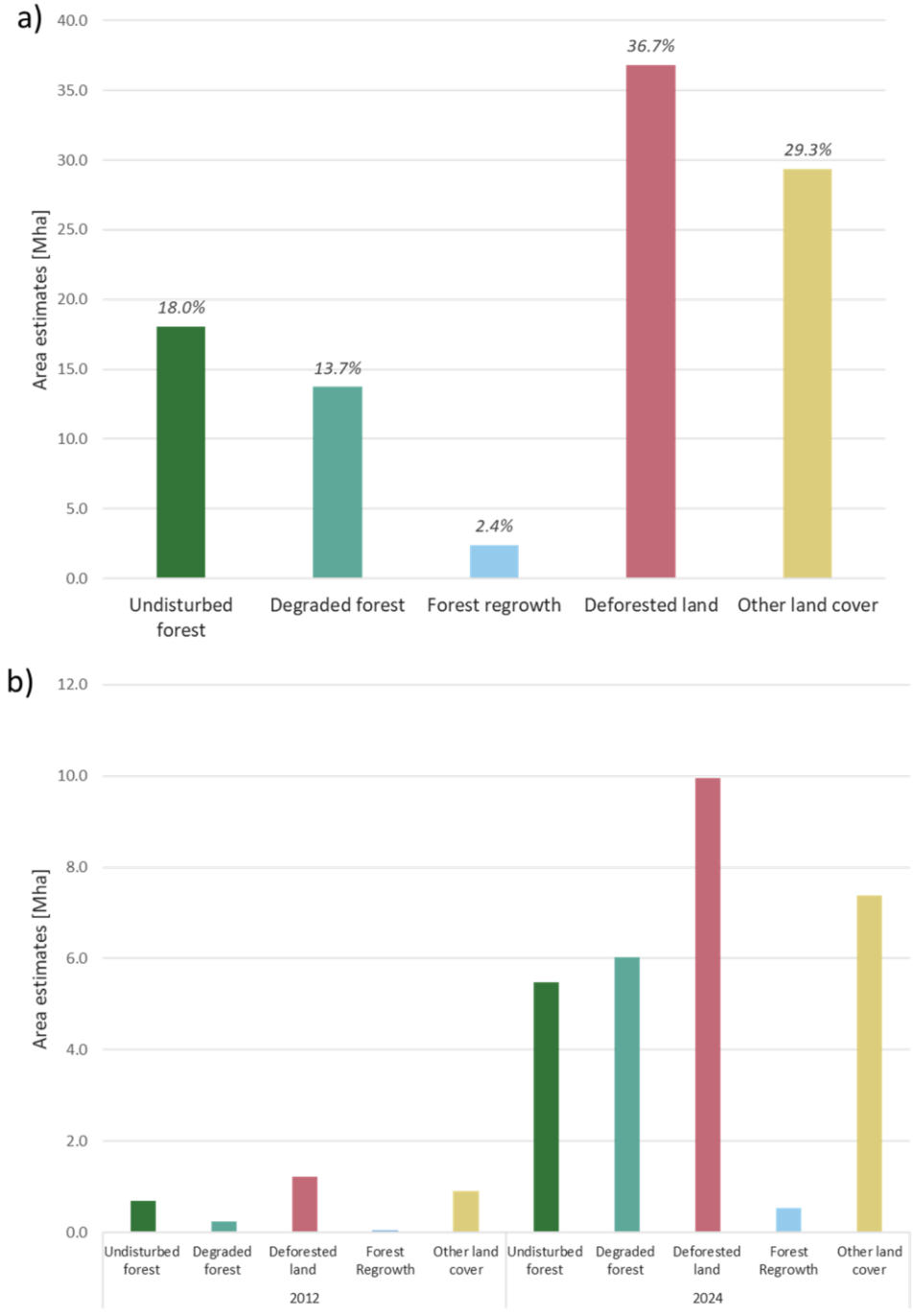


**Figure A3:** (a) Total thermal anomalies (2012–2024) from GWIS, distributed across TMF transition classes: undisturbed forest, degraded forest, forest regrowth, deforested land (detected between 1990 and 2024), and other land cover (including areas deforested prior to 1990). (b) Annual GWIS thermal anomalies for 2012 and 2024, categorized by TMF annual land cover status, including undisturbed forest, degraded forest, deforested land, forest regrowth, and other land cover types in each respective year.

### A4 Estimation of $CO_2$ emissions and uncertainty analysis

We estimated carbon dioxide ($CO_2$) emissions resulting from fire-driven degradation and deforestation in the Amazon basin for the years 2022, 2023, and 2024 using a Monte Carlo simulation framework. Emissions were calculated based on spatially explicit data on change areas and aboveground biomass (AGB) from the 2021 ESA CCI AGB map (Santoro et al., 2024), incorporating uncertainty in all relevant variables, including classification errors in change areas. Burned forest areas from fire-driven degradation were identified through the spatial intersection of TMF forest degradation and GWIS fire detections (as detailed in the "Integration of TMF–GWIS datasets" section), enhancing confidence in the detection of burned forests while yielding a conservative estimate. Areas of deforestation were directly derived from TMF. For computational efficiency and to minimize the influence of spatial autocorrelation in AGB errors, we aggregated change areas (fire-driven degradation and deforestation), AGB, and its associated standard deviation within spatial units of 0.5-degree grid cells.

#### A4.1 Emissions from forest fires

Emissions from fire-affected areas ($E_{fire}$) were calculated using equation 1, which follows equation 2.27 of the 2006 IPCC guidelines (IPCC 2006) and factors from Table 2.5 and 2.6 of the 2019 IPCC (IPCC 2019):

$$E_{fire} = \sum_{i=1}^{n} A_i^{fire} \cdot B_i \cdot C_c \cdot G_{ef} \cdot 10^{-3} \quad (1)$$

where $A_i^{fire}$ is the adjusted burned forest area (ha) in spatial unit $i$, $B_i$ the aboveground biomass (Mg ha$^{-1}$) in spatial unit $i$, $C_c$ the combustion completeness (adimensional), $G_{ef}$ the emission factor (g $CO_2$ kg$^{-1}$ dry biomass), $n$ the number of spatial units, and $10^{-3}$ just converts g $CO_2$ to Mg $CO_2$. The emission factor $G_{ef}$ was sampled from a normal distribution with a mean of 1580 g $CO_2$ kg$^{-1}$ dry biomass and a standard deviation of 90 g $CO_2$ kg$^{-1}$ dry biomass, based on Andreae and Merlet (2001). Combustion completeness ($C_c$) was modeled as a normal distribution with a mean of 0.50 and standard deviation of 0.03, consistent with values reported for tropical forest fires (van der Werf et al., 2010).

#### A4.2 Emissions from deforestation

Emissions from deforestation ($E_{defor}$) were computed with equation 2:

$$E_{defor} = \sum_{i=1}^{n} A_i^{defor} \cdot B_i \cdot C \cdot \left(\frac{44}{12}\right) \quad (2)$$

where $A_i^{defor}$ is the adjusted deforested area (ha), $C$ the carbon fraction of dry biomass (fixed at 0.47), 44/12 the molecular weight ratio to convert carbon to $CO_2$. Unlike fire emissions, no combustion completeness or emission factor is needed for deforestation, as it is assumed that all biomass is eventually emitted (IPCC, 2006).

### A4.3 Uncertainty in area estimates

To incorporate classification uncertainty in both burned and deforested area estimates, we applied probabilistic adjustments to the mapped areas using commission and omission error rates derived from the confusion matrix reported in Vancutsem et al. (2021). These error rates were modelled as Beta distributions to reflect their probabilistic nature, enabling their integration into a Monte Carlo simulation framework. This approach follows best practices for area estimation under classification uncertainty (Olofsson et al., 2014). Specifically, commission error was modelled as $Beta(\alpha_{cm} = 8.4, \beta_{cm} = 91.6)$, and omission error as $Beta(\alpha_{om} = 18.1, \beta_{cm} = 81.9)$. These distributions were used to adjust the mapped areas of burned and deforested land in each simulation iteration, allowing uncertainty in classification accuracy to propagate into the final emissions estimates. Adjusted areas ($A^{adj}$) were computed in each iteration of the simulation using equation 3:

$$A^{adj} = \frac{A \cdot (1 - e_c)}{1 - (e_c + e_o)} \quad (3)$$

where $e_c$ and $e_o$ are sampled commission and omission errors, respectively.

### A4.4 Monte Carlo simulation

We performed 100,000 Monte Carlo iterations per year and source. In each iteration, we simultaneously sampled i) commission and omission errors (affecting area adjustments), ii) AGB values (modeled as normal distributions with mean and standard deviation derived from the data), combustion completeness and emission factor for fire emissions only. Negative samples were truncated at zero. The result was a distribution of total $CO_2$ emissions for each source (fire, deforestation) and year, from which the average and standard deviation were derived.

## Code availability

Codes used for running the spatial statistics were written in javascript and R and are available upon request from the corresponding author.

## Data availability

All data used to download tropical moist forest disturbances and calculate its trends over the period 2001-2024 from the Tropical Moist Forest (TMF) dataset are accessible via: https://forobs.jrc.ec.europa.eu/TMF. All data used to download the fire detections and calculate their trends are from the Global Wildfire Information System (GWIS) dataset and are accessible via: https://gwis.jrc.ec.europa.eu/.

## Author contributions

CB: Conceptualization; formal analysis; investigation; methodology; writing – original draft. RB: Conceptualization; methodology; writing – review and editing. AB: Conceptualization; writing – review and editing. JC: Conceptualization; investigation; methodology; writing – review and editing. GC: Conceptualization; writing – review and editing. DO: Conceptualization; methodology; writing – review and editing. JSMA: Conceptualization; methodology; writing – review and editing. FS: Conceptualization; methodology; writing – review and editing.

## Competing interests

The authors declare that they have no conflict of interest.

## Disclaimer

The views expressed are purely those of the writers and may not in any circumstances be regarded as stating an official position of the European Commission. Publisher's note: Copernicus Publications remains neutral with regard to jurisdictional claims made in the text, published maps, institutional affiliations, or any other geographical representation in this paper. While Copernicus Publications makes every effort to include appropriate place names, the final responsibility lies with the authors.

## Acknowledgements

We are grateful for technical support, feedback and comments received during numerous discussions from Frédéric Achard, Rene Colditz, Andrea Marelli, Silvia Carboni, Dario Simonetti and Mirco Migliavacca. The authors utilized AI tools to enhance the readability of this work. Following its use, the authors thoroughly reviewed and edited the content as necessary and took full responsibility for the content of the manuscript.

## Financial support

Clément Bourgoin and João Carreiras are supported by the Amazonia+ Administrative Arrangement of the European Commission. The Global Wildfire Information System (GWIS) is supported by the Copernicus Work Program.

## Review statement

This paper was edited by Sara Vicca and reviewed by two anonymous referees.

**References**


Andela, N., Morton, D. C., Schroeder, W., Chen, Y., Brando, P. M., Randerson, J. T.: Tracking and classifying Amazon fire events in near real time, Sci. Adv.8, eabd2713, https://doi.org/10.1126/sciadv.abd2713, 2022.

Andreae, M. O., Merlet, P.: Emission of trace gases and aerosols from biomass burning, Global Biogeochemical Cycles, 15(4), 955–966, https://doi.org/10.1029/2000GB001382, 2001.

Barlow, J., Berenguer, E., Carmenta, R., França, F.: Clarifying Amazonia's burning crisis, Glob. Chang. Biol. 26, 319–321, https://doi.org/10.1111/gcb.14872, 2020.

Beuchle, R., Achard, F., Bourgoin, C., Vancutsem, C., Eva, H., Follador, M.: Deforestation and forest degradation in the Amazon - Status and trends up to year 2020, EUR 30727 EN, Publications Office of the European Union, Luxembourg, ISBN 978-92-76-38352-9, https://doi.org/10.2760/61682, 2021.

Birant, D., Kut, A.: ST-DBSCAN: An algorithm for clustering spatial–temporal data, Data & Knowledge Engineering, Volume 60, Pages 208-221, https://doi.org/10.1016/j.datak.2006.01.013, 2007.

Bourgoin, C., Ceccherini, G., Girardello, M., Vancutsem, C., Avitabile, V., Beck, P. S. A., Beuchle, R., Blanc, L., Duveiller, G., Migliavacca, M., Vieilledent, G., Cescatti, A., Achard, A.: Human degradation of tropical moist forests is greater than previously estimated, Nature 631, 570–576, https://doi.org/10.1038/s41586-024-07629-0, 2024.

Cano-Crespo, A., Oliveira, P. J. C., Boit, A., Cardoso, M., Thonicke, K.: Forest edge burning in the Brazilian Amazon promoted by escaping fires from managed pastures, J. Geophys. Res. Biogeosci., 120, 2095–2107, https://doi.org/10.1002/2015JG002914, 2015.

Condé, T. M., Higuchi, N., Lima, A. J. N.: Illegal Selective Logging and Forest Fires in the Northern Brazilian Amazon, Forests, 10, 61, https://doi.org/10.3390/f10010061, 2019.

Eva, H., Huber, O.: A Proposal for defining the geographical boundaries of Amazonia, EUR 21808 EN, Luxembourg, Office for Official Publications of the European Communities, JRC68635, 2005.

Flores, B. M., Montoya, E., Sakschewski, B., Nascimento, N., Staal, A., Betts, R. A., Levis, C., Lapola, D. M., Esquível-Muelbert, A., Jakovac, C., Nobre, C. A., Oliveira, R. S., Borma, L. S., Nian, D., Boers, N., Hecht, S. B., ter Steege, H., Arieira,

J., Lucas, I. L., Berenguer, E., Marengo, J. A., Gatti, L. V., Mattos, C. R. C., Hirota, M.: Critical transitions in the Amazon forest system, Nature 626, 555–564, https://doi.org/10.1038/s41586-023-06970-0, 2024.

Friedlingstein, P., O'Sullivan, M., Jones, M. W., Andrew, R. M., Hauck, J., Landschützer, P., Le Quéré, C., Li, H., Luijkx, I. T., Olsen, A., Peters, G. P., Peters, W., Pongratz, J., Schwingshackl, C., Sitch, S., Canadell, J. G., Ciais, P., Jackson, R. B., Alin, S. R., Arneth, A., Arora, V., Bates, N. R., Becker, M., Bellouin, N., Berghoff, C. F., Bittig, H. C., Bopp, L., Cadule, P., Campbell, K., Chamberlain, M. A., Chandra, N., Chevallier, F., Chini, L. P., Colligan, T., Decayeux, J., Djeutchouang, L. M., Dou, X., Duran Rojas, C., Enyo, K., Evans, W., Fay, A. R., Feely, R. A., Ford, D. J., Foster, A., Gasser, T., Gehlen, M., Gkritzalis, T., Grassi, G., Gregor, L., Gruber, N., Gürses, Ö., Harris, I., Hefner, M., Heinke, J., Hurtt, G. C., Iida, Y., Ilyina, T., Jacobson, A. R., Jain, A. K., Jarníková, T., Jersild, A., Jiang, F., Jin, Z., Kato, E., Keeling, R. F., Klein Goldewijk, K., Knauer, J., Korsbakken, J. I., Lan, X., Lauvset, S. K., Lefèvre, N., Liu, Z., Liu, J., Ma, L., Maksyutov, S., Marland, G., Mayot, N., McGuire, P. C., Metzl, N., Monacci, N. M., Morgan, E. J., Nakaoka, S.-I., Neill, C., Niwa, Y., Nützel, T., Olivier, L., Ono, T., Palmer, P. I., Pierrot, D., Qin, Z., Resplandy, L., Roobaert, A., Rosan, T. M., Rödenbeck, C., Schwinger, J., Smallman, T. L., Smith, S. M., Sospedra-Alfonso, R., Steinhoff, T., Sun, Q., Sutton, A. J., Séférian, R., Takao, S., Tatebe, H., Tian, H., Tilbrook, B., Torres, O., Tourigny, E., Tsujino, H., Tubiello, F., van der Werf, G., Wanninkhof, R., Wang, X., Yang, D., Yang, X., Yu, Z., Yuan, W., Yue, X., Zaehle, S., Zeng, N., and Zeng, J.: Global Carbon Budget 2024, Earth Syst. Sci. Data, 17, 965–1039, https://doi.org/10.5194/essd-17-965-2025, 2025.

Hirota, M., Flores, B. M., Betts, R., Borma, L. S., Esquível-Muelbert, A., Jakovac, C., Lapola, D. M., Montoya, E., Oliveira R. S., Sakschewski, B.: Chapter 24: Resilience of the Amazon Forest to Global Changes: Assessing the Risk of Tipping Points, https://doi.org/10.55161/QPYS9758, 2021.

IPCC. 2006 IPCC Guidelines for National Greenhouse Gas Inventories Vol. 4 (eds Eggleston, S. et al.) (IGES, 2006), 11, 2006.

IPCC. 2019 Refinement to the 2006 IPCC Guidelines for National Greenhouse Gas Inventories Vol. 4 (eds Buendia, E. C. et al.), 2019.

Justice, C. O., Giglio, L., Korontzi, S., Owens, J., Morisette, J. T., Roy, D., Descloitres, J., Alleaume, S., Petitcolin, F., Kaufman, Y.: The MODIS fire products, Remote Sensing of Environment, Volume 83, Issues 1–2, Pages 244-262, ISSN 0034-4257, https://doi.org/10.1016/S0034-4257(02)00076-7, 2002.

Kornhuber, K., Bartusek, S., Seager, R., Schellnhuber, H. J., Ting, M.: Global emergence of regional heatwave hotspots outpaces climate model simulations, Proc. Natl. Acad. Sci. U.S.A. 121 (49) e2411258121, https://doi.org/10.1073/pnas.2411258121, 2024.

Lapola, D. M., Pinho, P., Barlow, J., Aragão, L. E. O. C., Berenguer, E., Carmenta, R., Liddy, H. M., Seixas, H., Silva, C. V. J., Silva-Junior, C. H. L., Alencar, A. A. C., Anderson, L. O., Armenteras, D., Brovkin, V., Calders, K., Chambers, J., Chini, L., Costa, M. H., Faria, B. L., Fearnside, P. M., Ferreira, J., Gatti, L., Gutierrez-Velez, V. H., Han, Z., Hibbard, K., Koven, C., Lawrence, P., Pongratz, J., Portela, B. T. T., Rounsevell, M., Ruane, A. C., Schaldach, R., da Silva, S. S., von Randow, C., Walker, W. S.: The drivers and impacts of Amazon forest degradation, Science 379, eabp8622, https://doi.org/10.1126/science.abp8622, 2023.

Lima, T. A., Beuchle, R., Griess, V. C., Verhegghen, A., Vogt, P.: Spatial patterns of logging-related disturbance events: a multi-scale analysis on forest management units located in the Brazilian Amazon, Landscape Ecol 35, 2083–2100, https://doi.org/10.1007/s10980-020-01080-y, 2020.

Matricardi, E. A. T., Skole, D. L., Pedlowski, M. A., Chomentowski, W.: Assessment of forest disturbances by selective logging and forest fires in the Brazilian Amazon using Landsat data, International Journal of Remote Sensing, 34(4), 1057–1086, https://doi.org/10.1080/01431161.2012.717182, 2012.

Marengo, J., Cunha, A., Espinoza, J., Fu, R., Schöngart, J., Jimenez, J., Costa, M., Ribeiro, J., Wongchuig, S., Zhao, S.: The Drought of Amazonia in 2023-2024, American Journal of Climate Change, 13, 567-597, https://doi.org/10.4236/ajcc.2024.133026, 2024.

Melo, J., Baker, T., Nemitz, D., Quegan, S., Ziv, G.: Satellite-based global maps are rarely used in forest reference levels submitted to the UNFCCC, Environmental Research Letters 18, 034021, https://doi.org/10.1088/1748-9326/acba31, 2023.

Morton, D. C, DeFries, R. S., Nagol, J., Souza, C. M., Kasischke, E. S., Hurtt, G. C., Dubayah, R.: Mapping canopy damage from understory fires in Amazon forests using annual time series of Landsat and MODIS data, Remote Sensing of Environment, Volume 115, Issue 7, Pages 1706-1720, ISSN 0034-4257, https://doi.org/10.1016/j.rse.2011.03.002, 2011.

Olofsson, P., Foody, G. M., Herold, M., Stehman, S. V., Woodcock, C. E., Wulder, M. A.: Good practices for estimating area and assessing accuracy of land change. Remote Sensing of Environment, 148, 42–57, https://doi.org/10.1016/j.rse.2014.02.015, 2014.

Rorato, A. C, Escada, M. I. S., Camara, G., Picoli, M. C. A., Verstegen, J. A.: Environmental vulnerability assessment of Brazilian Amazon Indigenous Lands, Environmental Science & Policy, Volume 129, Pages 19-36, ISSN 1462-9011, https://doi.org/10.1016/j.envsci.2021.12.005, 2022.

Santoro, M.; Cartus, O.: ESA Biomass Climate Change Initiative (Biomass_cci): Global datasets of forest above-ground biomass for the years 2010, 2015, 2016, 2017, 2018, 2019, 2020 and 2021, v5.01, NERC EDS Centre for Environmental Data Analysis, https://doi.org/10.5285/bf535053562141c6bb7ad831f5998d77, 2024.

San-Miguel, J., Durrant, T., Suarez-Moreno, M., Oom, D., Branco, A., Libertà, G., De Rigo, D., Ferrari, D., Roglia, E., Scionti, N., Maianti, P., Boca, R., Broglia, M., Callisaya, F., Cerezo, R., Monasterios, G., Santos, L. Q., Claure, A., Nobrega De Oliveira, L., Senra De Oliveira, M., Terra, G., Morita, J. P., Marcon Silva, M., Setzer, A., Morelli, F., Libonati, R., Bernini, H., Lobos Stephani, P. A., Saavedra Salinas, J. A., Brull Badia, J., Garzon Cadena, N., Arenas Aguirre, M. A., Avila, K., Solano, L., Lancheros, S., Puerto Prieto, J. C., Jader Ocampo, J., Vargas Hernandez, M., Gonzalo Murcia, U., Arias, J., Rodriguez Leon, A., Moreno, L. M., Diana, S., Pazmiño, J., Cobos, S., Segura, D., Herrera, X., Sarango, C., Quispillo, M., Arrega Diaz, C., Cruz, E., Salgado, T., Toffoletti, M., Pereira Gavilan, R., Alarco Basaldua, G. E., Zarella Pequeño Saco, T., Epiquien Rivera, J. L., Canales Campos, W. L., Liza Contreras, R. A., Ricalde Bellido, C., Zubieta Barragan, R., Saavedra Estrada, R. M., Sono Alba, S., Ramirez Arroyo, R., Diaz Escobal, E., Albornoz Yañez, M., Casaretto Gamonal, M., Rosas, G., Quispe, N., Gonzales Figueroa, J., Cueva Melgar, E. L., Salinas, C., Ocampo, I., Ruffino, M., Riaño, R., Rico, S. and Escudero, P., Forest Fire Information and Management Systems in Latin America and the Caribbean, European Union Publications Office, Luxembourg, https://doi.org/10.2760/454551, JRC134498, 2023.

Schroeder, W., Oliva, P., Giglio, L., Csiszar, I. A.: The New VIIRS 375m active fire detection data product: Algorithm description and initial assessment, Remote Sensing of Environment, Volume 143, Pages 85-96, ISSN 0034-4257, https://doi.org/10.1016/j.rse.2013.12.008, 2014.

van der Werf, G. R., Randerson, J. T., Giglio, L., Collatz, G. J., Mu, M., Kasibhatla, P. S., Morton, D. C., DeFries, R. S., Jin, Y. J, van Leeuwen, T. T.: Global fire emissions and the contribution of deforestation, savanna, forest, agricultural, and peat fires (1997–2009), Atmospheric Chemistry and Physics, 10(23), 11707–11735. https://doi.org/10.5194/acp-10-11707-2010, 2010.

Vancutsem, C., Achard, F., Pekel, J. F., Vieilledent, G., Carboni, S., Simonetti, D., Gallego, J., Aragão, L. E. O. C., and Nasi, R.: Long-Term (1990–2019) Monitoring of Forest Cover Changes in the Humid Tropics, Science Advances 7 (10): eabe1603, https://doi.org/10.1126/sciadv.abe1603, 2021.